Dynamic Behaviour Analysis of Optical Linear Encoder under Mechanical Vibrations

Donatas GURAUSKIS*, Artūras KILIKEVIČIUS**

Department of Mechanical Engineering, Vilnius Gediminas Technical University, J. Basanavičiaus 28, 03224 Vilnius, Lithuania, E-mail: donatas.gurauskis@vgtu.lt
**Institute of Mechanical Science, Vilnius Gediminas Technical University, J. Basanavičiaus 28, 03224 Vilnius, Lithuania, E-mail: arturas.kilikevicius@vgtu.lt*

1. Introduction

Optical linear encoders play noticeable role in performance of computer numerical controlled machines (CNC) [1], coordinate measuring machines (CMM), robotics [2], positioning stages [3], tracking systems [4] and other precision positioning applications [5]. Usually, the accuracy of technological process, performed by the equipment, depends on the used encoder`s accuracy. It is obvious that the good performance of the encoder is very important.

In practice, mechanical vibrations are one of the factors which cause errors in linear displacement measurement encoders. Resonance in measuring device parts like aluminium extrusion or reading head, either in supporting elements of the application could cause additional undesirable motion of a scanning carriage (cursor) along a measuring scale. Such motion inevitably affects accuracy. Essentially, dynamic behaviour of the encoder depends on its construction. J. López et al. investigates the behaviour of the linear encoder under vibrations based on different optical scanning methods [6,7], and encoder`s errors under vibration at different mounting conditions [8]. Although, there are developed methodologies to evaluate optical encoders performance under vibration [9] or compensate vibration caused errors [10], but in order to have a good understanding of ongoing processes in mechanical construction of each encoder, more detailed investigation such as modal analysis is required.

In this paper, the dynamic behaviour of enclosed type optical encoder based on reflective light modulation is investigated. Its dynamic response to external mechanical excitation, generated by the electrodynamic shaker, is recorded by accelerometers and the most precarious resonant frequencies are determined. In order to establish how the encoder elements, behave at these resonances, the modal analysis is done.

2. Experimental details

The optical linear encoder analysed in this work is incremental. It is reflective type and its measuring scale is fabricated on the stainless-steel tape surface by a laser. This provides the opportunity to reach measuring length up to 30 meters. Meanwhile, encoders with a glass scale reach approximately about 3 meters. In cases when encoder`s length must be more than 2 meters, several of modular aluminium extrusions are added together. Stainless-steel tape with an engraved measuring scale is fitted into encoder`s aluminium extrusion, respectively stretched by using a special spring-

based mechanism and tightened at both ends. Another stainless-steel tape is used as a guideway for the precise scanning carriage positioning and motion during the displacement measurement process. Main parts of the tested linear encoder are shown in Fig. 1.
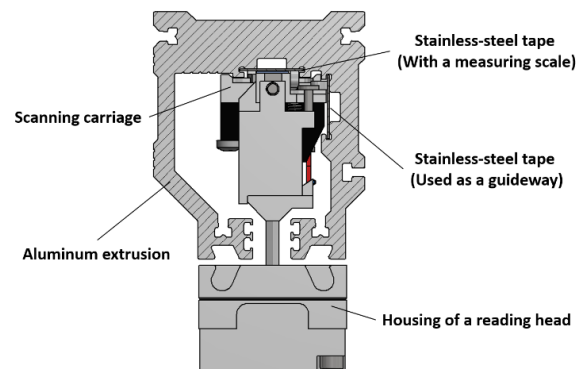
Fig. 1 Construction of tested linear encoder

The main idea of this experimental research is to analyse dynamic behaviour and determine resonant frequencies which could cause errors of the encoder. Theoretically, errors appear due to additional undesirable motion between the measuring scale and the reticle, mounted onto the scanning carriage. Even a small motion or oscillation generates electrical signals, which incorrectly represent the real displacement value.

Because the most important motion is along the measuring scale, the dynamic responses of the encoder`s aluminium extrusion and reading head are investigated only in this direction (meet the y axis in Fig. 2). Linear encoder is tightly mounted onto the laboratory table in such way, that its reading head has no ability to move with regard to aluminium extrusion. Two piezoelectric accelerometers are respectively mounted on top of the extrusion and housing of the reading head. Massive electrodynamic shaker is positioned close to the encoder to generate external mechanical excitation with the amplitude of about 100 mm/s^2 at each frequency. It imitates vibrations that occur in real applications. Excited encoder`s parts start to oscillate. When shaker generated excitation frequency is getting closer to the resonant frequencies of the encoder`s elements, the oscillation amplitudes increase. These resonant frequencies are the most dangerous, because the encoder starts to generate some kind of electric signals, even though there is no wanted displacement to measure. Despite the fact that the accuracy is directly affected, high frequency oscillations, caused by vibrations, remains during the displacement measurement

process. This generates higher harmonics and the analogue encoder signals become distorted. Interpolation process of such encoder signals is disturbed, and higher resolution becomes hardly reachable. The composition of the experimental setup is shown in Fig. 2.
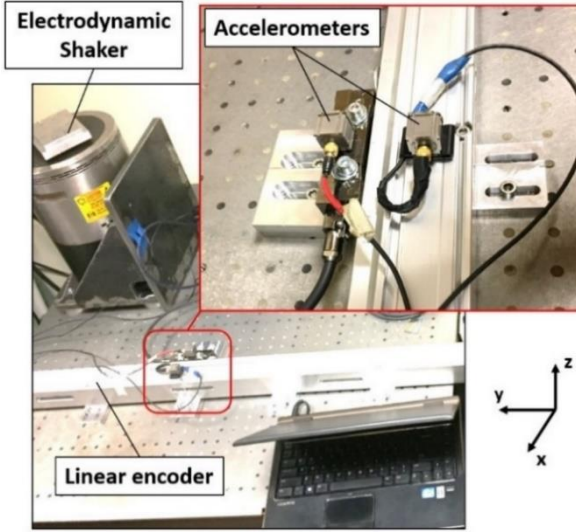
Fig. 2 Experimental setup used for encoder investigation

In order to reveal encoder`s behaviour and determine resonant frequencies, the device is tested under the sweep of sine wave form vibrations. Later, the amplitudes of aluminium extrusion and reading head responses under various resonant and other frequencies are measured. The biggest differences between the recorded amplitude values of oscillating elements distinguish excitations, which potentially generate the biggest errors. To check it, electrical 1 V peak-to-peak encoder`s output signals are recorded by a digital oscilloscope during the all experiment.

Used experimental equipment consists of:

1. Processing equipment. Data acquisition hardware "B&K" 3660-163D.

2. Electrodynamic shaker. Head "B&K" 4812, permanent magnet body "B&K" 4805, and amplifier "B&K" 2707.

3. Accelerometers. 3-axis piezoelectric accelerometer "B&K" 4506.

4. Data acquisition and processing equipment. Digital oscilloscope "PicoScope" 3000 and notebook.

The schematic representation of the experimental setup is shown in Fig. 3.
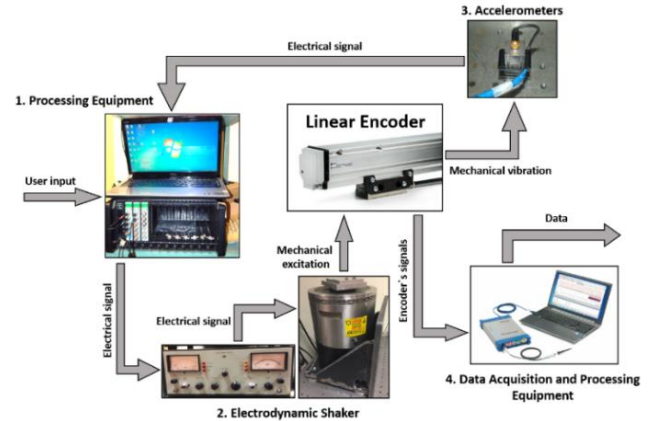
Fig. 3 Schematic representation of experimental setup

At each resonance mechanical elements oscillate in different manner. Modal analysis shows the oscillation shape of the elements. This simulation is performed by using the finite element method (FEM) in a computer software "COMSOL". A simplified 3D model of the encoder is created and divided into finite number of free tetrahedral (tets) elements with a predefined extra fine size. Boundary conditions such as fixing points of extrusion and reading head imitates encoder`s mounting in real application.

A simplified 3D model is shown in Fig. 4. Materials and their mechanical properties for each one of simulated device elements are listed in Table 1.
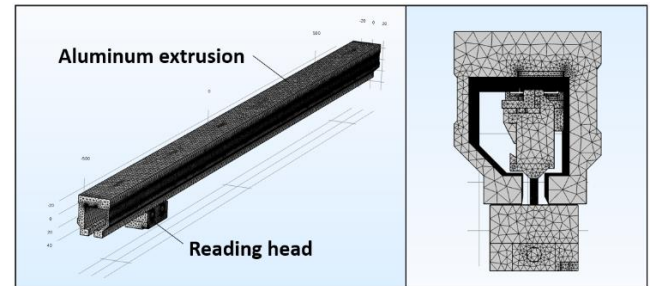
Fig. 4 Simplified 3D encoder model for FEM simulation

Table 1

Materials and mechanical properties of encoder elements

Element	Material	Mechanical properties		
		Density ρ, kg/m³	Young's modulus E, GPa	Poisson's ratio ν
Extrusion	Aluminum 6060	2700	70	0,33
Reading head	Aluminum 6082T6	2700	69	0,33
Measuring scale	Stainless-steel AISI 420	7700	190	0,28
Springs (reading head suspension)	Stainless-steel AISI 302	7800	200	0,28

Optical encoder generates two sinusoidal output signals S_A and S_B. They should have same size amplitudes A_A and A_B, zero offset from background level $(B_A = B_B = 0)$ and must be shifted by 90 electrical degrees $(\varphi_B - \varphi_A = \pi/2)$. These signals could be mathematically expressed as:

$$S_A = A_A F_A\left(2\pi \frac{x}{p} + \varphi_A\right) + B_A, \quad (1)$$

$$S_B = A_B F_B\left(2\pi \frac{x}{p} + \varphi_B\right) + B_B, \quad (2)$$

where: F_A, F_B is the shape (sinusoidal) of the signals; x is the position and p is the period.

The linear displacement could be easily determined according these signals by using arctangent algorithm:

$$x_{arctan} = \frac{p}{2\pi} arctan\left(\frac{S_A}{S_B}\right). \tag{3}$$

Output signals could be visually represented by the Lissajous curve. The curve appears in an oscilloscope screen, when one signal is plotted against another in x and y axis. Full circular shape corresponds to a relative motion between the reticle and the measuring scale, which is equal to a period of raster elements on them. The period of the tested encoder`s scale is 40 μm. Typically, external mechanical vibration initiates smaller motion between the optical components than one period. In case, when the reading head is mounted in fixed position as well as the aluminum extrusion, generated output signals are presented as a circumference arc of the Lissajous curve. From the size of arc, it is possible to determine and the size of error, generated by an external mechanical vibration.

During the displacement measurement process, encoder`s generated signals have multiple periods, so it is hard to exactly determined the amount of dynamic error. However, a specific mode shapes of the encoder mechanical components lead to a gap or tilt variation between the reticle and the glass scale. Disturbed optical interaction could present a loss of contrast and uneven light distribution on surfaces of used photodiodes. These variations make changes in signals` amplitudes, phase, offsets and even the shape.

Metrological errors presented in optical linear encoder could be determined by analysing the Lissajous curve and its distortion from an ideal shape [11]. The following equations are derived to evaluate these errors.

$$U_{off}(x) = \frac{p}{2\pi} cos\left(\frac{2\pi}{p}x\right)\frac{\Delta B}{A}, \tag{4}$$

$$U_{amp}(x) = \frac{p}{4\pi} sin\left(4\pi\frac{x}{p}\right)\frac{\Delta A}{A}, \tag{5}$$

$$U_{phase}(x) = \frac{p}{2\pi} cos^2\left(\frac{2\pi}{p}x\right)\Delta\varphi, \tag{6}$$

$$U_{shape}(x) = \frac{p}{2\pi} sin\left(8\pi\frac{x}{p}\right)\Delta T, \tag{7}$$

where: U_{off}, U_{amp}, U_{phase} and U_{shape} stand for metrological errors respectively caused by signal offset, variation of amplitudes, phase shift and not sinusoidal shape of the signals.

Other conditions for these formulas: $A_B = A$; $A_A = A + \Delta A$; $B_A = \Delta B$; $\varphi_A = \Delta\varphi$; $\varphi_B = \pi / 2$.

3. Results and discussion

Firstly, encoder's response to sine sweep vibration test is done. The shaker is set to generate sinusoidal excitation from 0 to 3200 Hz. Collected data from the accelero-
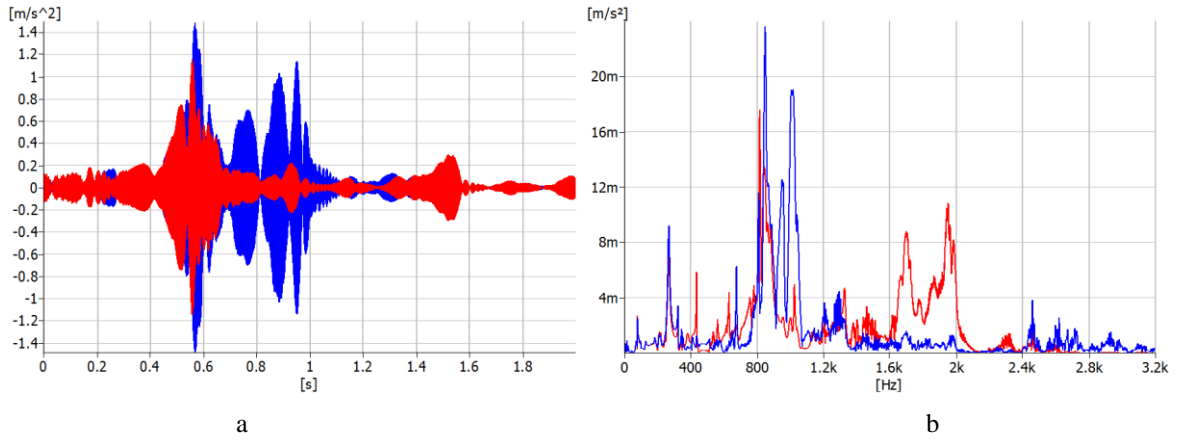
Fig. 5 Response graphs: a) acceleration amplitude versus time, b) auto-spectrum. (Aluminium extrusion response – blue line; reading head response – red line)
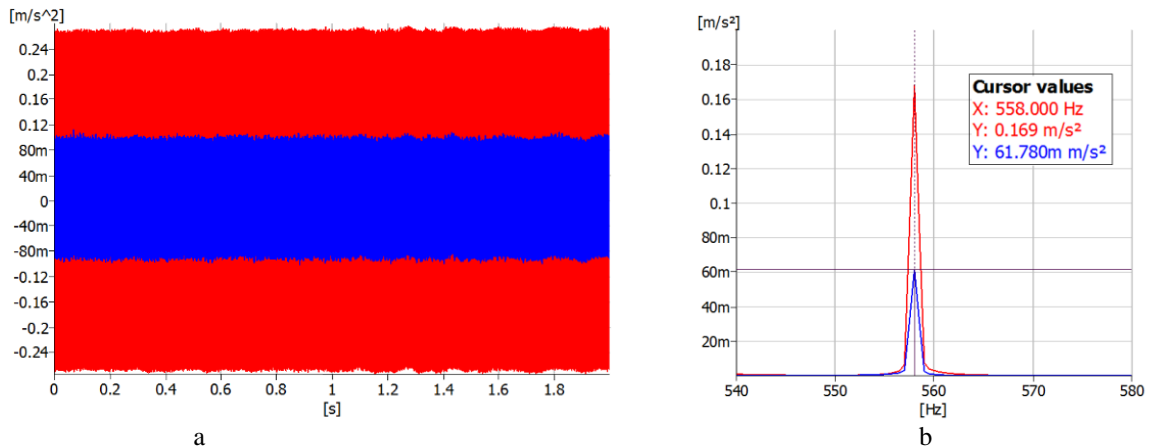
Fig. 6 Response to 558 Hz excitation graphs: a) acceleration amplitudes versus time, b) auto-spectrum. (Aluminium extrusion response – blue line; reading head response – red line)

meters presents the frequency response of the aluminium extrusion and the reading head. Acceleration amplitude versus time and auto-spectrum graphs are plotted in Fig. 5. Resonant frequencies 382, 433, 534, 558, 629,5, 753 and 815,5 Hz are selected for more detailed investigation.

Secondly, linear encoder is excited with a discrete sine vibration up to 2000 Hz with a step of 100 Hz, including selected resonant frequencies. The values of frequency response amplitudes are recorded by the accelerometers. For example, aluminium extrusion and reading head responses to 558 Hz selected resonant frequency are shown in Fig. 6.

In this case the acceleration amplitude of the reading head oscillations reaches 169 mm/s^2 and the extrusion oscillates at 61,78 mm/s^2. The difference between amplitudes is almost three times.

According measured amplitude values the revised graphs of frequency responses to sine wave form mechanical vibration are plotted. The graph composed for the reading head is shown in Fig. 7.

Several sharp peaks could be clearly seen in this graph. According the accomplished modal analysis, some of these peaks quite accurately correspond to the determined modes. They are marked on the graph. Other modes may not have such clearly visible effect at investigated direction y. Oscillation modes: 1, 2, 3 and 6 are depicted in Fig. 8. Only the reading head and its mode shapes are shown in these images for a better visualization. It is obvious, that all excludedmodes are related to the motion of the scanning carriage and occur at tested frequencies of 433, 558, 815,5 and about 2000 Hz. Mechanical assembly and encoder`s mounting type could also change and the dynamic behaviour, so resonant frequencies of simulated modes and modes of the real encoder may slightly differ. Another graph composed of the aluminum extrusion response data is shown in Fig. 9.
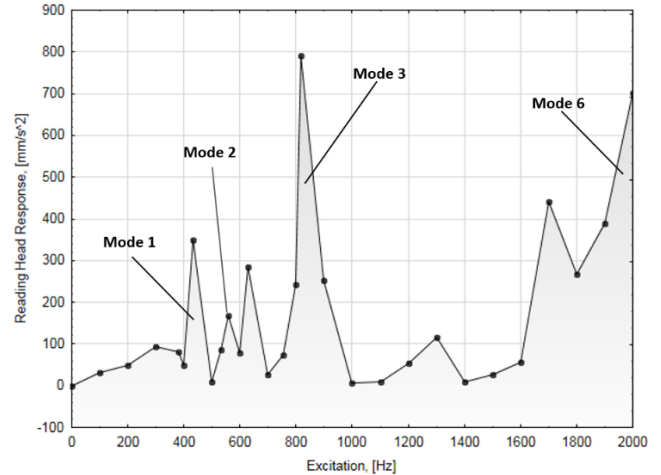
Fig. 7 Reading head frequency response graph with marked modes
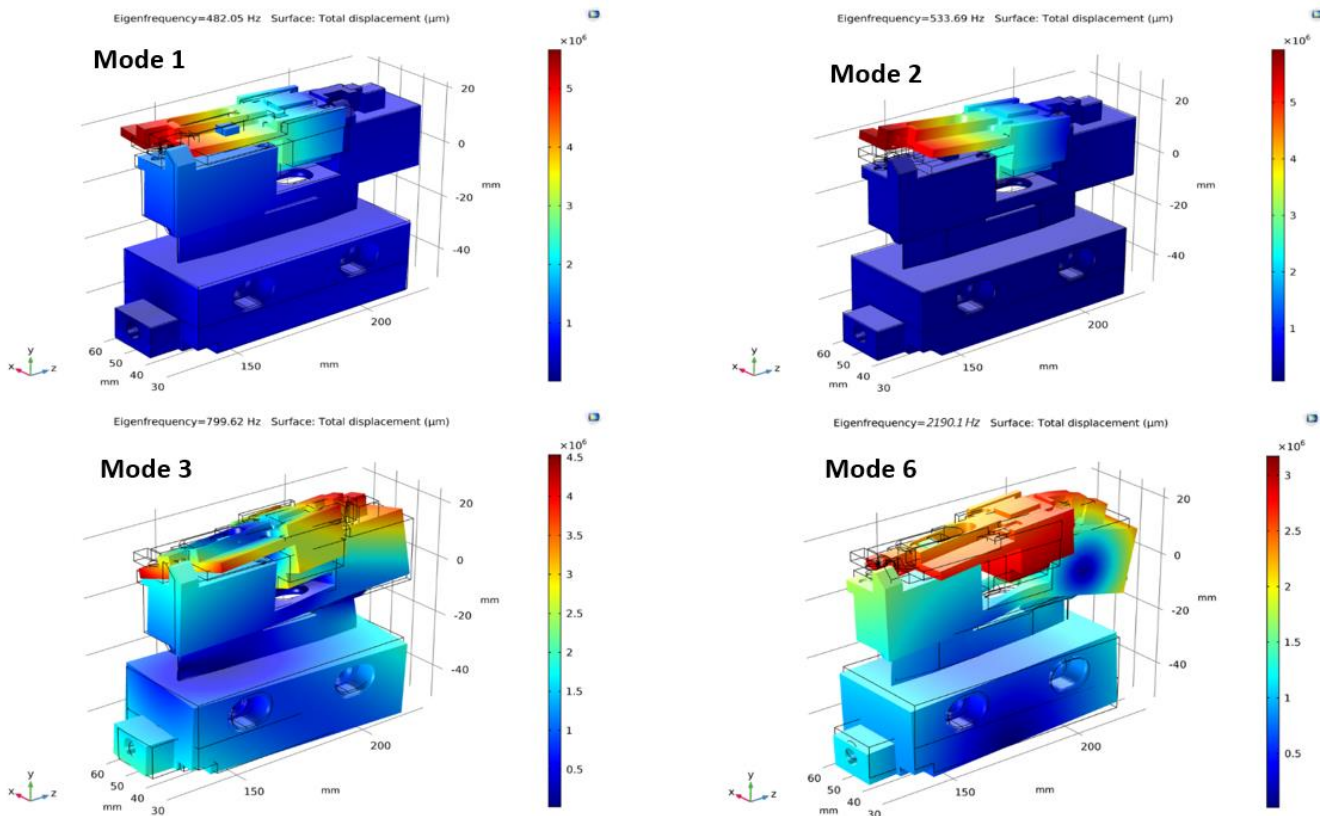
Fig. 8 Mode shapes of encoder`s reading head

Noticeable peaks correspond to the simulated modes: 7, 12, 13, 15 and 19. The shapes of these modes could be seen in Fig. 11. The swell type motion of the aluminum extrusion (mode 7 and mode 13) and the stainless-steel tape with a measuring scale (mode 12, mode 15 and mode 19) is generated at frequencies of 300, 800, 900, 1200 and 1700 Hz respectively. Other peaks seen in both discussed graphs could appear due to resonances of the experimental setup or the synergetic effect of the other factors.

When the oscillation amplitude values of the aluminum extrusion and the reading head are similar at the same frequency, the motion between the main optical com-
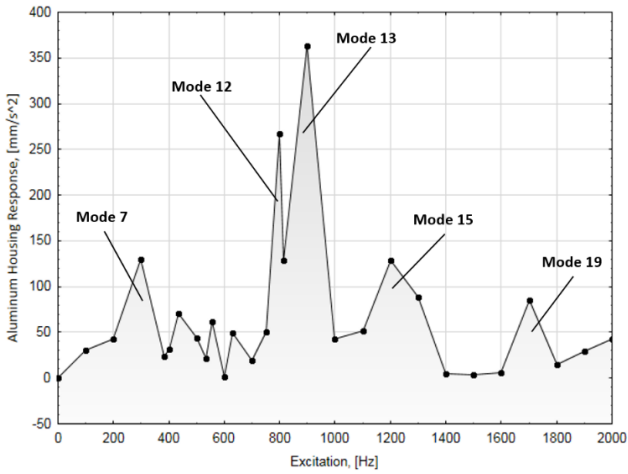
Fig. 9 Aluminum extrusion frequency response graph with marked modes
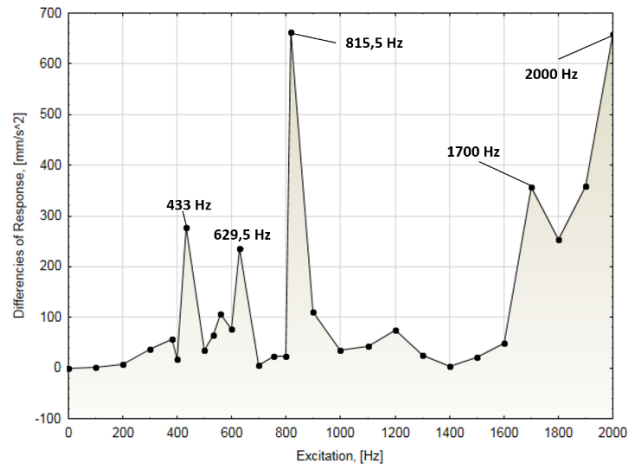
Fig. 10 Differences between response amplitude values of reading head and aluminum extrusion
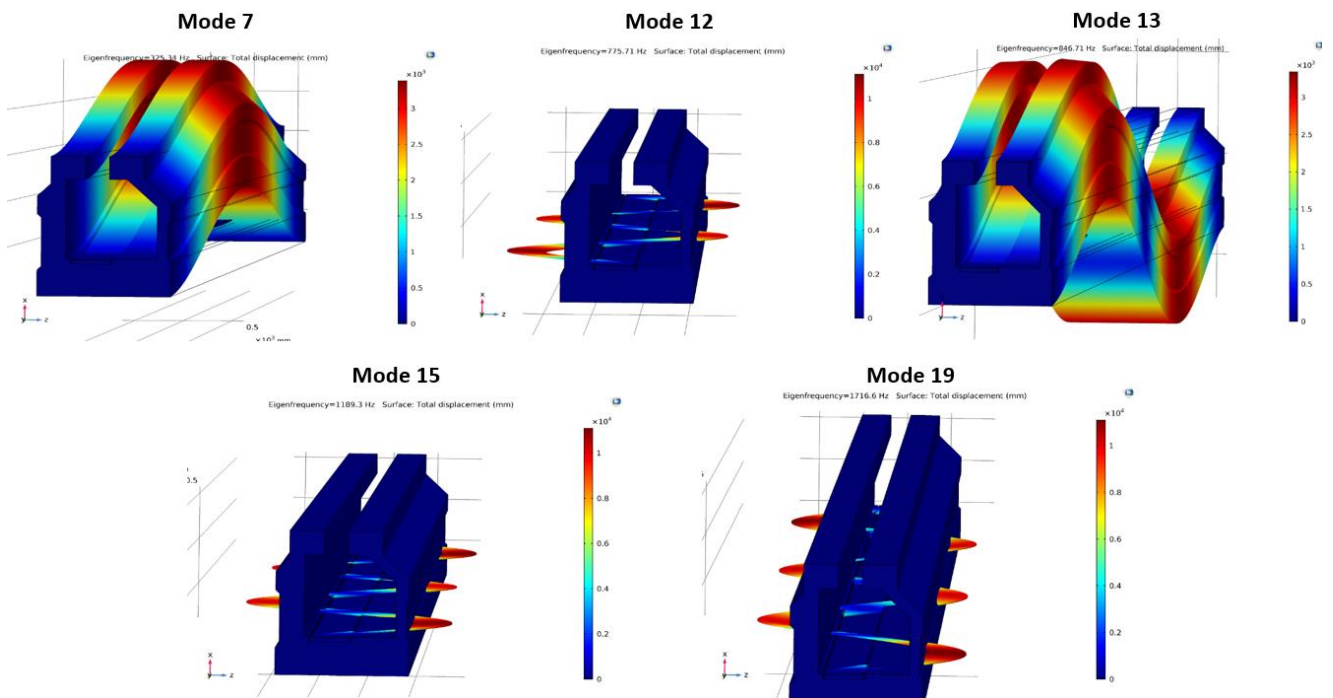
Fig. 11 Mode shapes of encoder`s aluminum extrusion
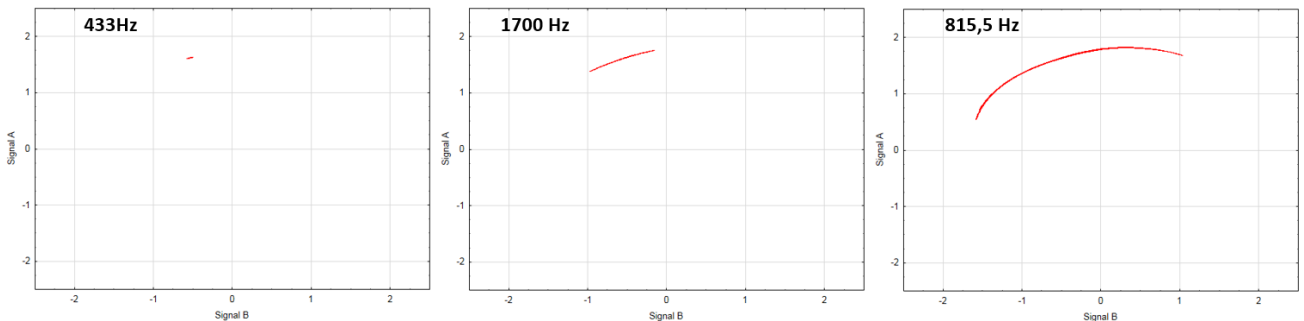
Fig. 12 Circumference arcs of Lissajous curves at 433, 1700 and 815,5 Hz

ponents is relatively small, even then the amplitude values are big. Much bigger relative motion appears in cases, when one of the elements oscillates with appreciably bigger amplitude. The differences between the response amplitudes are plotted in Fig. 10.

This graph shows potentially the most dangerous

frequencies which could generate displacement measurement errors. The peaks appear at 433; 629,5; 815,5; 1700 and 2000 Hz.

In order to check the influence of these resonant frequencies the electric output signals generated by the encoder are analyzed. Three examples of Lissajous curves of

electrical signals recorded at 433; 815,5 and 1700 Hz are shown in Fig. 12. The corresponding arcs show that encoder`s performance under vibration is affected. The generated error reaches <1 μm at 433 Hz; ~4 μm at 1700 Hz and ~11 μm at 815,5 Hz.

Electrical signals are recorded and during the displacement measurement process, to see how external mechanical excitation affects its performance. The Lissajous curve of working encoder under 815,5 Hz excitation is shown in Fig. 13.
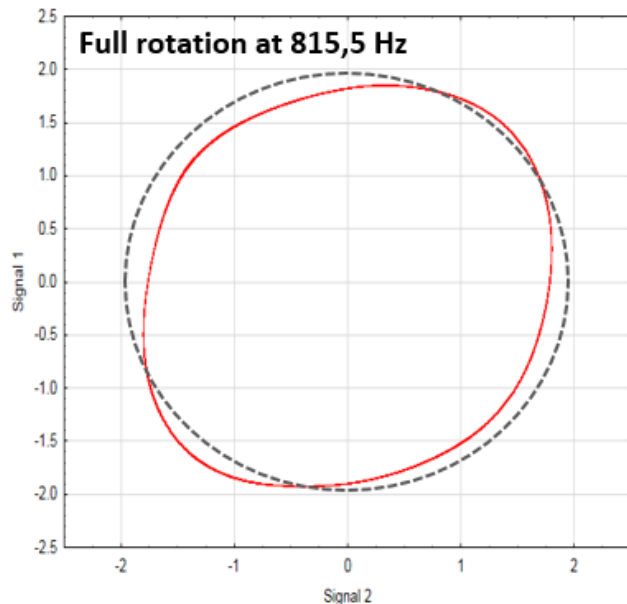
Fig. 13 Lissajous curve of working encoder under 815,5 Hz mechanical excitation (Lissajous curve of the tested encoder - solid red line; ideal circular curve – dashed black line)

Properly working linear encoder generates good quality sin and cos signals. The Lissajous curve of such signals looks like almost perfect circle. The graph above shows that the electrical signals are distorted. Shape of the curve are not circular and represents uneven amplitudes of electric signals. Slightly non-centered elliptical shape configuration tells about the phase distortion and different offsets of the output signals.

4. Conclusions

In this study, the dynamic behaviour of the linear optical encoder under mechanical vibrations is analysed. The main resonant frequencies and corresponding mode shapes of the encoder`s elements are determined. Potentially the most dangerous frequencies, which could cause the biggest displacement measurement errors are distinguished.

The results could be summarized as follow:

1) Accomplished sine sweep vibration test shows that there are resonant frequencies in the studied frequency range. Motion of the reading head along the encoder`s measuring scale is considered as the most dangerous and is selected like a point of interest in this work.

2) Determined resonances generate errors up to ~11 μm. Accuracy of the encoder is ±10 μm/m by itself. This means that mechanical vibrations can significantly worsen the performance of the tested device.

3) The Lissajous curve of working encoder under vibrations shows that analogue electrical signals are distorted. Amplitudes, offsets and phase of the signals vary during the displacement measurement process. This is usually related to a tilt or air gap variations between the reticle and the measuring scale. It means, that not only the forward and backward oscillations are generated.

4) Determined mode shapes expose that the biggest errors are generated due to the swell type motion of the aluminum extrusion and the stainless-steel tape. They are also directly related to a various motion of the scanning carriage.

5) In order to improve encoder performance under mechanical vibrations, changes in mechanical design of the reading head may help to reduce resonant frequencies. Especially it is important to do in a range from 50 to 2000 Hz, which is mentioned in standard EN 60068-2-6 (sinusoidal vibrations). Most linear encoders must support conditions according this standard.

Due to various mounting types and different length of aluminum extrusion, it is hard to describe its exact dynamic behaviour. However, the stainless-steel tape in all cases are relatively stretched and fixed on both ends. Considering such encoder`s construction, the following steps could be discussed to improve its dynamic behaviour under vibrations:

1) The harder stretch of the stainless-steel tape may increase the stiffness of the assembly and as a consequence, the resonant frequencies should become higher. To achieve this, raster elements of the incremental track should be made with a correspondingly corrected period.

2) Depending on the length of the aluminum extrusion assembly, several additional fixing pins could be integrated into design. These pins could be respectively placed to press a tape at points, where its modal shape reaches maximal peaks.

Unfortunately, these cases require changes in encoder`s mechanical design or the technological process of scale engraving. Either way, more detailed experimental investigation is required.

References

1. **Alejandre I.; Artés M.** 2004. Machine tool errors caused by optical linear encoders, Journal of Engineering Manufacture 218(1): 113-122.
   https://doi.org/10.1243/095440504772830255.

2. **Rodriguez-Donate, C.; Osornio-Rios, R. A.; Rivera-Guillen, J. R.; Romero-Troncoso, J.** 2011. Fused smart sensor network for multi-axis forward kinematics estimation in industrial robots, Sensors 11(4): 4335-4357.
   https://doi.org/10.3390/s110404335.

3. **ChaBum, L.; Gyu, H. K.; Sun-Kyu, L.** 2011. Design and construction of a single unit multi-function optical encoder for a six-degree-of-freedom motion error measurement in an ultraprecision linear stage, Meas. Sci. Technol. 22(105901): 8.
   https://doi.org/10.1088/0957-0233/22/10/105901.

4. **Chong, K.; Wong, C.; Siaw, F.; Yew, T.; Ng, S.; Liang, M.; Lim, Y.; Lau, S.** 2009. Integration of an on-axis general sun-tracking formula in the algorithm of an open -loop sun-tracking system, Sensors 9: 7849-7865.
   https://doi.org/10.10.3390/s91007849.

5. **Gao, W.; Kim, S. W.; Bosse, H.; Haitjema, H.; Chen,**

Y. L.; Lu, X. D.; Knapp, W.; Weckenmann, A.; Estler, W.T.; Kunzmann, H. 2015. Measurement technologies for precision positioning, Manufacturing technologies 64(2): 773-796.
https://doi.org/10.1016/j.cirp.2015.05.009.

6. **López, J.; Artés, M.; Alejandre, I.** 2012. Analysis under vibrations of optical linear encoders based on different scanning methods using an improved experimental approach, Experimental techniques 36(6): 35-47.
https://doi.org/10.1111/j.1747-1567.2011.00749.x.

7. **López, J.; Artés, M.; Alejandre, I.** 2009. Vibration behaviour analysis of optical linear encoders based on different scanning methods. Proceeding of the SEM Annual Conference. Society for Experimental Mechanics Inc.

8. **López, J.; Artés, M.; Alejandre, I.** 2011. Analysis of optical linear encoders` errors under vibration at different mounting conditions, Measurement 44(8): 1367-1380.
https://doi.org/10.1016/j.measurement.2011.05.004.

9. **Alejandre, I.; Artés, M.** 2007. Method for the evaluation of optical encoders performance under vibration, Precision Engineering 31(2): 114-121.
https://doi.org/10.1016/j.precisioneng.2006.03.004.

10. **López, J.; Artés, M.** 2012. A new methodology for vibration error compensation of optical encoders, Sensors 12(4): 4918-4933.
https://doi.org/10.3390/s12040491.

11. **Sanchez-Brea, L. M.; Morlanes, T.** 2008. Metrological errors in optical encoders, Measurement Science and Technology 19(115104): 8.
https://doi.org/10.1088/0957-0233/19/11/115104.

D. Gurauskis, A. Kilikevičius

DYNAMIC BEHAVIOUR ANALYSIS OF OPTICAL LINEAR ENCODER UNDER MECHANICAL VIBRATIONS

S u m m a r y

Mechanical vibrations are probably inevitable and occur in more or less all machine tools and other technological equipment. In case the linear encoder is used for moveable parts positioning in such machines, vibrations could cause additional errors. This paper investigates the dynamic behaviour of the optical linear encoder under mechanical vibrations. Potentially the most harmful frequencies are determined experimentally, and the corresponding mode shapes are simulated by using the finite element method (FEM). Obtained results describe tested encoder`s construction dynamic response to external excitation and could be used to improve its design.